Resonance Raman spectroscopy reveals new insight into the electronic structure of beta-hematin and malaria pigment

ARTICLE *in* JOURNAL OF THE AMERICAN CHEMICAL SOCIETY · AUGUST 2004

Impact Factor: 12.11 · DOI: 10.1021/ja038691x · Source: PubMed

J|A|C|S
ARTICLES
Published on Web 07/09/2004

Resonance Raman Spectroscopy Reveals New Insight into the Electronic Structure of β-Hematin and Malaria Pigment

Bayden R. Wood,*,† Steven J. Langford,† Brian M. Cooke,‡ Janelle Lim,† Fiona K. Glenister,‡ Martin Duriska,† Jessica K. Unthank,† and Don McNaughton†

Contribution from the Centre for Biospectroscopy, School of Chemistry, and the Department of Microbiology, Monash University, Victoria, 3800, Australia

Received September 24, 2003; E-mail: bayden.wood@sci.monash.edu.au

Abstract: Resonance Raman spectra of β-hematin and hemin are reported for a range of excitation wavelengths including 406, 488, 514, 568, 633, 780, 830, and 1064 nm. Dramatic enhancement of A_{1g} modes (1570, 1371, 795, 677, and 344 cm^{-1}), ring breathing modes (850−650 cm^{-1}), and out-of-plane modes including iron−ligand modes (400−200 cm^{-1}) were observed when irradiating with 780- and 830-nm laser excitation wavelengths for β-hematin and to a lesser extent hemin. Absorbance spectra recorded during the transformation of hemin to β-hematin showed a red-shift of the Soret and *Q* (0−1) bands, which has been interpreted as excitonic coupling resulting from porphyrin aggregation. A small broad electronic transition observed at 867 nm was assigned to a *z*-polarized charge-transfer transition $d_{xy} \rightarrow e_g(\pi^*)$. The extraordinary band enhancement observed when exciting with near-infrared excitation wavelengths in β-hematin when compared to hemin is explained in terms of an aggregated enhanced Raman scattering hypothesis based on the intermolecular excitonic interactions between porphyrinic units. This study provides new insight into the electronic structure of β-hematin and therefore hemozoin (malaria pigment). The results have important implications in the design and testing of new anti-malaria drugs that specifically interfere with hemozoin formation.

Introduction

Strategies for drug design in the treatment of malaria aim at producing effective, nontoxic, and inexpensive therapeutic agents for use in Africa, Asia, and South America, where the combined mortality rate is over one million per year.[1] A potential drug target is the lysosomal food vacuole of the parasite, where hemoglobin is degraded into the potentially toxic ferrous-protoporphyrin IX (Fe(II)PPIX), rapidly oxidized to ferric-protoporphyrin IX hydroxide also known as hematin (Fe-(III)PPIX-OH), and sequestered into an insoluble compound known as hemozoin or malaria pigment.[2−4] Powder diffraction data collected of β-hematin $(Fe(III)PPIX)_2$, a spectroscopically identical synthetic analogue of hemozoin,[4] obtained with synchrotron radiation have been examined and interpreted to be an array of dimers linked through reciprocal iron−carboxylate bonds to one of the propionate side chains and that these dimers in turn form chains linked by hydrogen bonds.[5]

Quinoline blood schizonticides such as chloroquine and quinine are thought to inhibit heme aggregation by binding to monomeric or dimeric hematin.[5] This results in higher concentrations of free heme in the food vacuole capable of inducing membrane lysis, especially when complexed to chloroquine.[6,7] Studies have shown that many antimalarial drugs accumulate in the food vacuole and exert their influence by binding to heme.[8−10] Consequently, knowledge of the formation of β-hematin and hemozoin as well as their structure has important implications in drug development and in understanding the heme−drug interactions occurring within the food vacuole of the mature parasites.

Raman spectroscopy has long provided structural information on porphyrin moieties in hemes and other metalloporphyrins in solution.[11] The high symmetry and chromophoric structure of hemes such as hemin (Fe(III)PPIX-Cl), depicted in Figure 1, result in strong Raman scattering upon excitation with different wavelengths. The early work of Tang and Albrecht[12] provided insight into the relationship between resonance Raman intensities and excited-state structure and determined that there

† Centre for Biospectroscopy and School of Chemistry.
‡ Department of Microbiology.

(1) Greenwood, B.; Mutabingwa, T. *Nature* **2002**, *415*, 670−672.
(2) Bohle, D. S.; Conklin, B. J.; Cox, D.; Madsen, S. K.; Paulson, S.; Stephens, P. W.; Yee, G. T. Structural and Spectroscopic Studies of β-Hematin (the Heme Coordination Polymer in Malaria Pigment). In *Inorganic and Organometallic Polymers II: Advanced Materials and Intermediates*; ACS Symposium Series 572; Wisian-Neilson, P., Allcock, H. R., Wynne, K. J., Eds.; American Chemical Society: Washington, DC, 1994, pp 497−515.
(3) Francis, S.; Sullivan, D. J.; Goldberg, D. *Annu. Rev. Micobiol.* **1997**, *51*, 97−123.
(4) Slater, A. F. G.; Swiggard, W. J.; Orton, B. R.; Flitter, W. D.; Goldberg, D.; Cerami, A.; Henderson, G. B. *Proc. Natl. Acad. Sci. U.S.A.* **1991**, *88*, 325−329.
(5) Pagola, S.; Stephens, P. W.; Bohle, D. S.; Kosar, A. D.; Madsen, S. K. *Nature* **2000**, *404*, 307−310.
(6) Fitch, C. D.; Chevli, R.; Banyal, H. S.; Phillips, G.; Pfaller, M. A.; Krogstad, D. J. *Antimicrob. Agents Chemother.* **1982**, *21*, 819−822.
(7) Ridley, R. G. *Exp. Parasitol.* **1997**, *87*, 293−304.
(8) Ridley, R. G. *Nature* **2002**, *415*, 686−693.
(9) Egan, T. J.; Hunter, R.; Kaschula, C. H.; Marques, H. M.; Misplon, A. *J. Med. Chem.* **2000**, *43*, 283−291.
(10) Egan, T. J.; Marques, H. M. *Coord. Chem. Rev.* **1999**, *192*, 493−517.
(11) Spiro, T. G.; Li, X.-Y. In *Biological Applications of Raman Spectroscopy*; Spiro, T. G., Ed.; Wiley: New York, 1988; Vol. 3, pp 1−38.

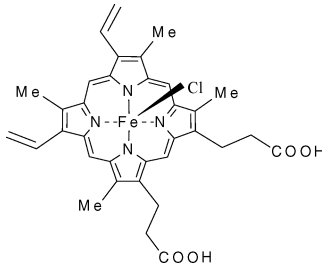

Figure 1. Structural formula of hemin.

are two important resonance Raman scattering terms. The type A enhancement depends on the product of the Franck−Condon integrals between the intermediate level and the initial and final vibrational states.[11] Only totally symmetric modes have nonzero values for this product, and hence they are involved in type A enhancement. For type B enhancement, the vibrational overlap also depends on the normal coordinate and can be nonzero for nontotally symmetric vibrations. In this case, a nearby strong allowed transition can enhance the intensity by vibronic mixing.[11]

Types A and B Raman scattering mechanisms serve as excellent models to explain resonance Raman spectra in dilute solutions. However, in the highly concentrated heme environment of malarial trophozoites, other factors such as excitonic interactions and degree of aggregation need to be considered. The exciton model is based on the quantum mechanical premise that electronic energy is distributed throughout the aggregate.[13] Aggregated enhanced Raman scattering (AERS) has been proposed to explain the anomalous enhancement observed in N-protonated porphyrins[14−16] and cyanine dyes absorbed onto surfaces.[13,17−20] The enhancement of vibrational modes can be explained in terms of an increase size effect and near-resonance terms in the polarizability.[13] Excitonic coupling will essentially split the electronic states into a broad band of states with different geometries, energies, and oscillator strengths. The Raman intensities for a particular wavelength will then reflect the extent of the excitonic coupling. Covalently linked porphyrin architectures including meso-meso-linked arrays of copper(II)[21,22] and zinc(II)[23] exhibit strong excitonic interactions showing a distinct splitting of the Soret band and unusual Raman scattering patterns. Depending on the model used to describe β-hematin, the propionate linkage between porphyrin units may also enable excitonic coupling, although to a lesser extent than meso-meso-linked arrays. Indeed, Raman spectra of hemozoin within the food vacuole of mature *Plasmodium falciparum* parasites within human erythrocytes have shown dramatic enhancement of totally symmetric modes including ν_4 (1376 cm^{-1}) observed when applying 780-nm excitation.[24] Moreover, this enhancement was used to generate Raman images of hemozoin within the food vacuole of malaria parasites in functional erythrocytes.[24]

In this study, β-hematin and hemin have been investigated using a variety of spectroscopic methods, including UV−visible, Fourier transform infrared (FTIR), and resonance Raman spectroscopy. The Raman excitation profiles presented for β-hematin and hemin show the enhancement of totally symmetric modes of heme moieties when exciting with laser lines in the near-IR region, including 780 and 830 nm. It is suggested the dramatic enhancement of totally symmetric modes observed at near-IR excitation wavelengths in β-hematin results from exciting into a *z*-polarized charge-transfer transition centered at 867 nm known as band I $d_{xz} \rightarrow e_g(\pi^*)$. The enhancement was shown to be greater in β-hematin compared to monomeric hemin, demonstrating that the stacking of hemes results in strong excitonic coupling for the near-IR charge-transfer (CT) *z*-polarized transition. The study provides new insights into the electronic structure of hemin, β-hematin, and malaria pigment.

Experimental Section

P. falciparum line 3D7[25] was maintained in continuous in vitro culture using human red blood cells suspended in HEPES-buffered RPMI-1640 media supplemented with 0.5% AlbumaxII as previously described[26] using standard procedures.[27] Cultures were used for experiments when the majority of parasites were pigmented trophozoites as assessed by examination of Giemsa stained smears. Hemozoin was extracted by applying the methodology adopted by Slater et al.[4] using 2×10^7 erythrocytes with parasitemias of 6−8% in the experiment.

Hemin was purchased from Sigma-Aldrich and Fluka and used as supplied for the majority of measurements. Hemin was also recrystallized using Koenig's method[28] and examined with 632.8- and 780-nm excitation wavelengths. Approximately 5 mg was transferred to an 80-mm Petri dish previously coated by evaporative deposition to produce an 80-nm aluminum layer. The Petri dish was then filled with 10 cm^3 of milli-Q water and placed into a temperature-controlled cell (Physitemp, TS-4LPD -large Petri dish stage) with a TS-4 thermoelectric controller (Physitemp) and cooled to 4 °C. The crystals were allowed to settle on the bottom of the Petri dish prior to spectral acquisition. Single crystals of the compound were targeted using a water immersion objective for spectral acquisition. For each spectrum, 10 scans were accumulated with a 10-s laser exposure time. Preparation of β-hematin was achieved using a number of previously described methods, all yielding similar results in terms of Raman excitation profiles.[29−31]

FTIR spectra of hemozoin and β-hematin were recorded with a DigiLab 7000 spectrometer coupled to a UMA 600 FTIR microscope. Samples were placed on Ag−SnO_2 slides, and spectra were recorded in reflection/absorption mode at 6 cm^{-1} resolution with 256 scans co-added.

UV−vis absorbance spectra were recorded during the acidification of hemin to form β-hematin using a Cary UV−visible spectrometer

(12) Tang, J.; Albrecht, A. C. In *Raman Spectroscopy*; Szymanski, H. A., Ed.; Plenum: New York, 1970; Vol. 2, pp 33−68.
(13) Akins, D. L.; Özcelik, S.; Zhu, H.-R.; Guo, C. *J. Phys. Chem.* **1997**, *101*, 3251−3259.
(14) Akins, D. L.; Özcelik, S.; Zhu, H.-R.; Guo, C. *J. Phys. Chem.* **1996**, *100*, 14390−14396.
(15) Akins, D. L.; Zhu, H.-R.; Guo, C. *J. Phys. Chem.* **1994**, *98*, 3612−3618.
(16) Akins, D. L.; Zhu, H.-R.; Guo, C. *J. Phys. Chem.* **1996**, *100*, 5420−5425.
(17) Akins, D. L.; Macklin, J. W. *J. Phys. Chem.* **1989**, *93*, 5999−6007.
(18) Akins, D. L.; Macklin, J. W.; Parker, L. A.; Zhu, H.-R. *Chem. Phys. Lett.* **1990**, *169*, 564−568.
(19) Akins, D. L.; Macklin, J. W.; Zhu, H.-R. *J. Phys. Chem.* **1991**, *95*, 793−798.
(20) Akins, D. L.; Zhuang, Y. H.; Zhu, H.-R.; Liu, J. Q. *J. Phys. Chem.* **1994**, *98*, 1068−1072.
(21) Bhuiyan, A. A.; Seth, J.; Yoshida, N.; Osuka, A.; Bocian, D. F. *J. Phys. Chem. B* **2000**, *104*, 10757−10764.
(22) Chen, D.-M.; Zhang, Y.-H.; He, T.-J.; Liu, F.-C. *Spectrochim. Acta* **2002**, *58*, 2291−2297.
(23) Kim, Y. H.; Jeong, D. H.; Kim, D.; Jeoung, S. C.; Cho, H. S.; Kim, S. K.; Aratani, N.; Osuka, A. *J. Am. Chem. Soc.* **2001**, *123*, 76−86.
(24) Wood, B. R.; Langford, S.; Cooke, B. M.; Glenister, F.; Lim, J.; Duriska, M.; McNaughton, D. *FEBS Lett.* **2003**, *554*, 247−252.
(25) Walliker, D.; Quakyi, I. A.; Wellems, T. E.; McCutchan, T.; et al. *Science* **1987**, *236*, 1661−1666.
(26) Cranmer, S. L.; Magowan, C.; Liang, J.; Coppel, R. L.; Cooke, B. M. *Trans. R. Soc. Trop. Med. Hyg.* **1997**, *91*, 363−365.
(27) Trager, W. *Methods Cell Biol.* **1994**, *45*, 7−26.
(28) Koenig, D. F. *Acta Crystallogr.* **1965**, *18*, 663−673.
(29) Blauer, G.; Akkawi, M. *J. Inorg. Biochem.* **1997**, *66*, 145−157.
(30) Bohle, D. S.; Helms, J. B. *Biochem. Biosphys. Res. Commun.* **1993**, *193*, 504−508.
(31) Egan, T. J.; Ross, D. C.; Adams, P. A. *FEBS Lett.* **1994**, *352*, 54−57.

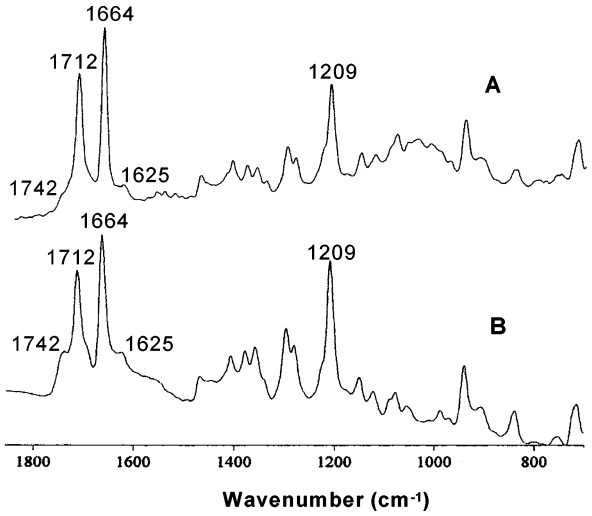

Figure 2. FTIR spectra of extracted hemozoin (A) and β-hematin (B), synthesized by the method of ref 30.

with automated stirrer at 293 K. A solution of hemin was prepared by dissolving 15 mg of hemin in 0.1 M NaOH (5 cm^3). This solution was gradually acidified by adding 10 μL of 1 M HCl every minute, and an absorption spectrum was recorded after each addition and subsequent mixing.

Raman spectra of β-hematin and hemin were recorded on a Renishaw system 2000 spectrometer using a 632.8 nm excitation line from a helium−neon laser and a 780-nm excitation line generated by a diode laser. The system is equipped with a modified BH2-UMA Olympus optical microscope and a Zeiss ×60 water immersion objective to enable spectral acquisition in water, thus minimizing the potential of thermal degradation of the hemin. It should be noted that the spectra of hemin were recorded of needlelike crystals individually targeted with the Raman microscope facility and not from amorphous powder residues. Other excitation wavelengths used included the 488- and 514-nm excitation lines generated by a Spectra Physics Ar^+ Stabilite 2017 laser system, a 568-nm excitation line generated by a Spectra-Physics Kr^+ Beamlock 2060 laser, and an 830-nm line from a diode laser. Spectra were also recorded using a 406-nm laser line generated by a krypton ion laser. In this configuration, all lasers were coupled to a Renishaw Raman 2000 spectrometer and interfaced to a Leica Raman microscope using the same water immersion objective as mentioned above except for the 406-nm spectrum, which was recorded using a conventional Olympus ×50 objective. Power at the sample was 2 ± 0.1 mW with a 1 to 2 μm laser spot size. Spectra were recorded between 1800 and 200 cm^{-1} with a resolution of ~1 to 2 cm^{-1}. For each spectrum, five scans were accumulated, and the laser exposure for each scan was 10 s except for the 406-nm spectrum, which was recorded in one 10 s accumulation. The laser exposure was interrupted between scans, while the grating repositioned to its starting position because constant exposure resulted in thermal degradation. FT-Raman spectra of β-hematin moistened with water were recorded on a Bruker FT-Raman spectrometer with a 1064-nm excitation line generated by an Nd:YAG laser. Power at the sample was 100 mW for 60 s.

Results

FTIR Spectroscopy. FTIR spectra of hemozoin extracted from mature pigmented *P. falciparum* parasites and β-hematin synthesized from hemin are compared in Figure 2. The spectra are similar to those previously reported[4,29] and clearly show bands at 1664 and 1209 cm^{-1} assigned to the carbonyl stretching mode and the C−O stretching vibration of the propionate linkage, respectively. The band at 1712 cm^{-1} is assigned to the hydrogen-bonded carboxylate group that is thought to link dimers together in the extended porphyrin array. The spectra show a previously unreported band at 1742 cm^{-1}, which appears as a pronounced shoulder in the spectrum of β-hematin and as a weak inflection in hemozoin. Second derivative analysis clearly resolved this band in both hemozoin and β-hematin. The spectra also exhibit a small band at 1625 cm^{-1}, which appears as a strong band in the Raman spectra at all excitation wavelengths investigated. This band, which is normally assigned to ν_{10} in the Raman spectrum, is therefore both Raman- and infrared-active.

UV−Vis Absorption Spectroscopy. The formation of β-hematin was monitored with optical spectroscopy by gradually acidifying a solution of hemin dissolved in 0.1 M NaOH and

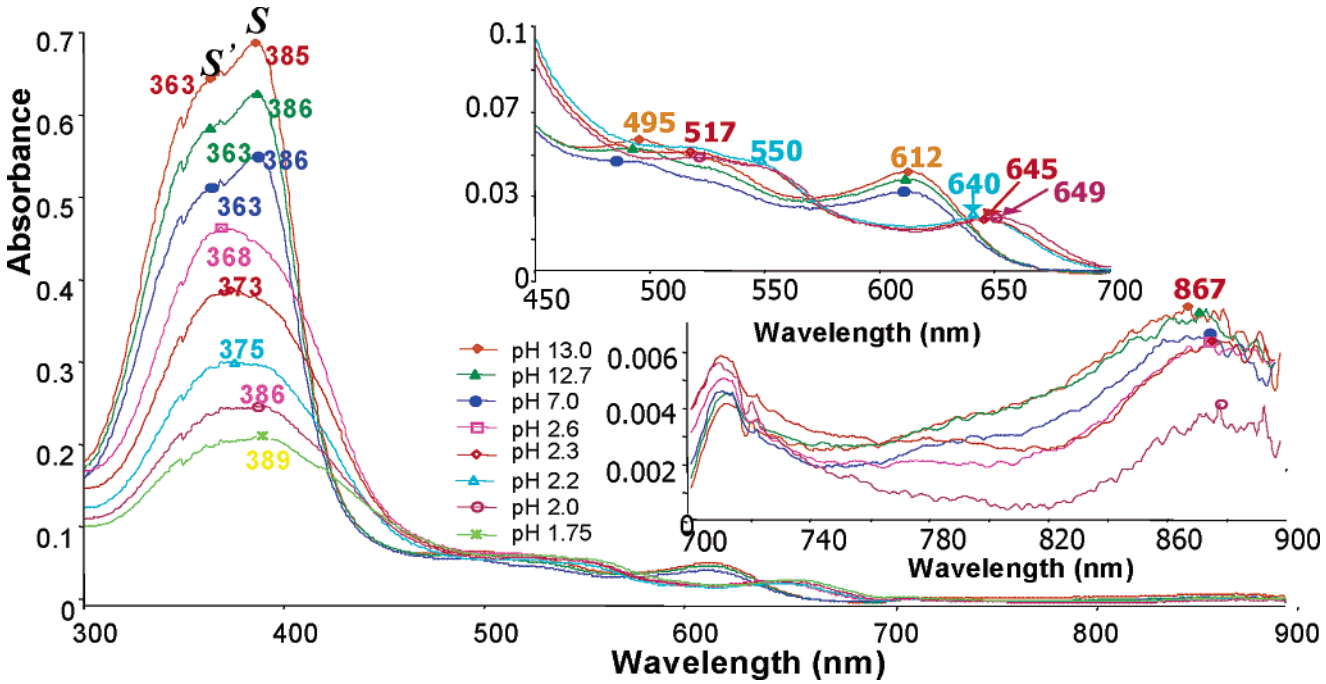

Figure 3. Absorbance spectra recorded during the acidification of hemin to form β-hematin.

recording absorbance spectra as a function of pH (Figure 3). The Soret band (or *B* band) in hemin is resolved into two bands appearing at 363 and 385 nm designated *S′* and *S*, respectively, along with *Q* bands at 495, 521, 550 (very weak), and 612 nm. The collapsing of the two Soret bands into one broad band centered at 389 nm along with the *Q* band at 649 nm observed at low pH discriminates β-hematin from hematin and hemin. Other bands observed in the absorbance spectrum of β-hematin include bands at 513 and 550 nm. The absorbance spectrum at low pH is similar to that recorded by Bohle et al.[2] of β-hematin measured as a potassium bromide pellet with reported bands at 406, 510, 538, and 644 nm. They also reported a band at 580 nm that is not observed in the solution spectra reported herein. The 649-nm band is characteristic of hemin aggregates[2] as determined by microspectrophotometry[32] and photoacoustic spectroscopy.[33] This band sequentially shifts (640, 645, 649 nm) as the pH decreases. For clarity, the spectra shown in Figure 3 represent the general trend and not the entire series. The decrease in pH broadens and reduces the intensity of the Soret band because of aggregation and precipitation of the β-hematin. The Soret band appears to red-shift from 363 to 389 nm; however, because of the broad nature of this band at low pH, accurate determination of the maxima is precluded. A red-shift in the Soret and Q-bands is indicative of excitonic coupling resulting from porphyrin aggregation.[21−23] It is interesting to note the small broad band centered at 867 nm in hemin and β-hematin. The band appears slightly red-shifted as the reaction proceeds and is also less intense in β-hematin than hemin, most likely as a result of the former precipitating as the reaction proceeds. This band has not previously been reported in the spectrum of either molecule and is tentatively assigned to a CT transition known as band I ($d_{xz} \rightarrow e_g(\pi^*)$).

Resonance Raman Spectroscopy. Figure 4 depicts Raman spectra collected of β-hematin using 406, 488, 514, 564, 633, 780, 830, and 1064-nm excitation wavelengths. The spectra of β-hematin are identical to the spectra recorded for hemozoin encapsulated within malarial infected cells at 488, 514, 564, 633, and 780 nm.[24] Spectra of hemin recorded using the same excitation wavelengths, except 1064 nm because this spectrum has previously been reported,[34] are presented in the Supporting Information.[35] Band assignments, local coordinates, and symmetry terms are also detailed in the Supporting Information.[36] To enable a direct comparison, all spectra presented in Figures 4 and 5 are normalized to ν_{10} (1625−1630 cm^{-1}) because this band appears intense at every excitation wavelength investigated, including nonresonant wavelengths such as 1064 nm. Excitation into the Soret band of hemin and β-hematin using the 406 nm laser line produces a classic type A (Franck−Condon) scattering pattern, showing the dramatic enhancement of several totally symmetric modes. These include bands at 1571−1570, 1491−1490, and 1373−1372 cm^{-1} assigned to ν_2, ν_3, and ν_4, all of A_{1g} symmetry. A number of low wavenumber bands associated

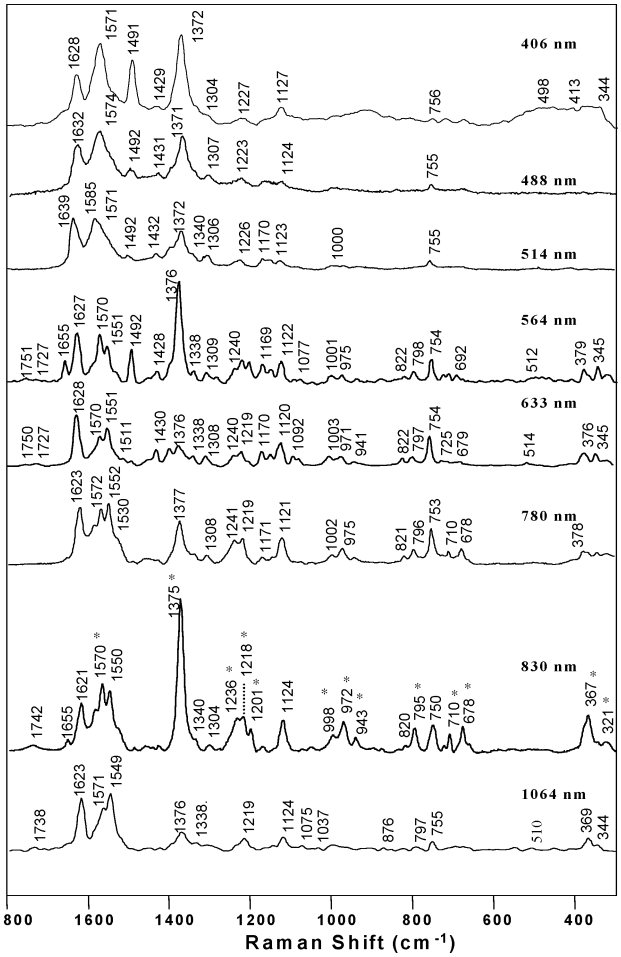

Figure 4. Raman spectra of β-hematin recorded using a variety of excitation wavelengths. The asterisks in the 830-nm spectrum highlight bands that appear dramatically enhanced.

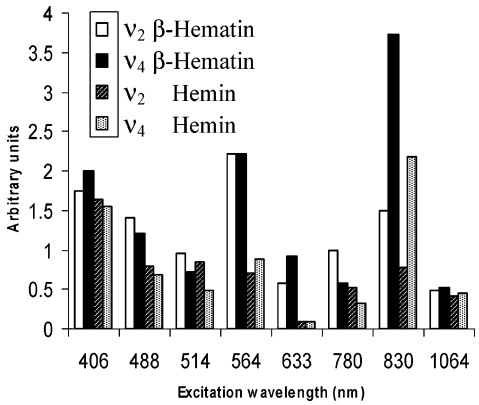

Figure 5. Raman intensity as a function of wavelength of β-hematin and hemin for the totally symmetric modes ν_2 and ν_4.

mainly with the out-of-plane and metal−ligand modes, including those at 526, 498, 413, 390, and 344 cm^{-1} also appear dramatically enhanced. The totally symmetric modes ν_2, ν_3, and ν_4 are also enhanced at 488 nm. These modes would be in preresonance with the Soret band at 400 nm, and thus the enhancement is also typical of a type A scattering. Excitation at 514 nm, which is close to the 515−521-nm *Q* (0−0) band, resulted in a decrease in relative intensity of the totally symmetric modes ν_2, ν_3, and ν_4. Bands at 1432−1428, 1307−1302, and 1170−1166 cm^{-1} in hemin were slightly more

(32) Morselt, A. F. W.; Glastra, A.; James *J. Exp. Parasitol.* **1973**, *33*, 17−22.
(33) Balasubramanian, D.; Rao, M. C.; Panijpan, B. *Science* **1984**, *223*, 828−830.
(34) Ozaki, Y.; Mizuno, A.; Sato, H.; Kawaguchi, K.; Muraishi, S. *Appl. Spectrosc.* **1992**, *46*, 533−535.
(35) The spectra of hemin crystals as supplied by Fluka and Sigma-Aldrich were compared with hemin recrystallized using Koenig's method (*Acta Crystallogr.* **1965**, 663−673), yielding very similar enhancement profiles for 633 and 780 nm excitation wavelengths.
(36) The heme compounds in this study have C_{4v} symmetry; however, D_{4h} notation is employed by convention.

pronounced at this wavelength compared to that at 488 nm. Exciting at 564 nm, which is close to the 550 nm *Q* (0,1) band in β-hematin, results in dramatically enhanced ν_2, ν_3, and ν_4 bands of A_{1g} symmetry. Other enhanced bands include 1551−1550, 1218 (β-hematin only), and 755 cm^{-1} assigned to ν_{11}, ν_{13}, and ν_{16}, all of B_{1g} symmetry. Pyrrole-breathing and deformation modes (800−600 cm^{-1}) along with out-of-plane modes (400−300 cm^{-1}) are also enhanced when exciting with 564 nm compared to 514- and 488-nm excitation wavelengths. Consequently, the spectrum has many features in common with the 406-nm spectrum. It is interesting to note the appearance of carbonyl bands at 1751 and 1727 cm^{-1}, which also appear in the 633-nm excitation spectrum of hemozoin. The spectrum also displays a small band appearing at 1655 cm^{-1}, which is close in wavenumber value to the 1662 cm^{-1} band observed in the FTIR spectrum of β-hematin and assigned by Slater et al.[4] to the carbonyl group of the propionate linker. This band is also observed when exciting with the 830-nm diode laser.

Excitation with 633 nm results in a dramatic decrease in the intensity of the ν_4 band along with bands at 1551 ($\nu_{11}-B_{1g}$) and 1570 cm^{-1} (ν_2-A_{1g}). However, the relative intensity of bands at 1233 ($\nu_{13}-B_{1g}$), 1124 ($\nu_{22}-A_{2g}$), 822 cm^{-1} and low wavenumber modes at 407, 377, 344, and 305 cm^{-1} all increase in intensity when exciting with 633-nm excitation. The increase in intensity of the bands that characterize the A_{2g} modes is consistent with scattering observed in the *Q* band excitation region where normally type B or Hertzberg−Teller scattering is the dominant mechanism. The Type A (or Franck−Condon) scattering term is not significant at these excitation wavelengths, and consequently the 1570- and 1370-cm^{-1} bands appear diminished. It is interesting to note the increase in intensity of the low wavenumber modes (500−300 cm^{-1}) compared to the spectra acquired using 488- and 514-nm excitation wavelengths. As mentioned above, these modes are generally attributed to out-of-plane porphyrin and axial modes.[37]

The 633-nm spectrum shows two small carbonyl bands at approximately 1750 and 1727 cm^{-1} that are also enhanced when applying 564-nm excitation. At longer excitation wavelengths (830 and 1064 nm), these bands appear to merge into one band centered at 1742 cm^{-1}, which corresponds in wavenumber value to the carbonyl band observed in the FTIR spectrum. Although this band is small, it is consistently reproduced in spectra recorded of β-hematin synthesized using different methods.

Enhancement at 780 nm is possibly due to preresonance with the small broad near-IR transition centered at 867 nm. The spectra recorded at this excitation wavelength and also at 830 nm show an extraordinary band enhancement profile compared to spectra recorded using 633 nm excitation. In particular, bands characteristic of totally symmetric A_{1g} modes including 1570, 1371, 795, 677(ν_6), and 344 cm^{-1} along with bands at 1552, 1220, and 755 cm^{-1} associated with B_{1g} modes have become dramatically enhanced. Figure 5 shows the Raman intensities of the totally symmetric modes ν_4 and ν_2 with respect to the normalization band ν_{10}. At 830-nm excitation, the intensity of the ν_4 band at 1371 cm^{-1} dominates the spectrum of β-hematin. The intensity of both ν_4 and ν_2 is greater in β-hematin than hemin for 830, 780, 564, and 488 nm. A number of low wavenumber modes are also dramatically enhanced at 780- and 830-nm excitation wavelengths, including bands at 821, 796, 752, 722, 710, and 678 cm^{-1}. FT-Raman spectra recorded of β-hematin using 1064-nm excitation show a dramatic reduction in the intensity of most of the totally symmetric modes including ν_4. This indicates that the 1064-nm excitation wavelength is now well away from the electronic transition responsible for the enhancement of these modes at 780- and 830-nm excitation.

Discussion

Mechanism of Enhancement. The appearance of intense A_{1g} modes in the Raman spectra of hemin and β-hematin when applying 780- and 830-nm excitation wavelengths is similar to the enhancement pattern observed in hemozoin encapsulated within functional erythrocytes.[24] Understanding the mechanism that enables totally symmetric modes to be dramatically enhanced in the 800−1000 nm requires interpretation of the absorption spectrum in this region. The optical absorption spectra recorded during the acidification of hemin to β-hematin at room temperature show two bands in the near-IR region. One small sharp band appears at 700 nm, together with a small broad band centered at 867 nm. The latter may provide some insight into the mechanism of this enhancement. High-spin ferric complexes such as hemin and β-hematin have an electronic ground state consisting of orbitally nondegenerate spin sextet $^6A_{1g}$. On the basis of extended Hückel theoretical calculations performed by Zerner et al.[38] on ferric high-spin porphine complexes including hemin and hematin, four charge-transfer transitions have been predicted. These involve promotions from the top four filled porphyrin π-orbitals into the degenerate d_{xz}, d_{yz} iron orbitals.[39] Polarized single-crystal absorption spectra showed that all four bands were *x*,*y*-polarized, therefore indicating the transitions are degenerate.[39] Magnetic circular dichroism (MCD) analysis of aquomethemoglobin indicated that a broad near-infrared band with an absorption maxima at 1040 nm contains two degenerate transitions at 1100 and 800 nm, which were also resolved in the fluoride complex and assigned to $a_{2u}(\pi) \rightarrow d_{xz},d_{yz}$ and $a_{1u}(\pi) \rightarrow d_{xz},d_{yz}$, respectively.[40] UV−vis spectra of tetraphenylporphyrin Fe(III) Cl recorded under vacuum on a thin layer optical cell clearly show an unassigned band at 870 nm.[41] Eaton and Holchester[39] identified a *z*-polarized band at 695 nm in ferricytochrome *c* and assigned it to the $a_{2u}(\pi) \rightarrow d_{z^2}$ transition. On the basis of symmetry considerations, the $a_{2u}(\pi) \rightarrow d_{z^2}$ is allowed, but the $a_{1u},a_{2u}(\pi) \rightarrow d_{x^2-y^2}$ pair is not.

Charge transfer can also take place from occupied d orbitals to vacant porphyrin $e_g(\pi^*)$ orbitals. Although this process is parity-forbidden, the restriction can be removed for hemes without an inversion center because of mixing in metal *p*-orbital character.[42] Figure 6 shows a qualitative molecular orbital diagram for the allowed transitions involving the Fe(III) and porphyrin orbitals for hemin based on the calculations of Zerner

(37) Hu, S.; Smith, K. M.; Spiro, T. G. *J. Am. Chem. Soc.* **1996**, *118*, 12638−12646.

(38) Zerner, M.; Gouterman, M.; Kobayashi, H. *Theor. Chim. Acta* **1966**, *6*, 363−399.

(39) Eaton, W. A.; Hochstrasser, R. M. *J. Chem. Phys.* **1968**, *49*, 985−995.

(40) Eaton, W. A.; Hofrichter, J. In *Hemoglobins*; Antonini, E., Rossi-Bernardi, L., Chiancone, E., Eds.; Academic Press: New York, 1981; Vol. 76, pp 175−261.

(41) Felton, R. H.; Owen, G. S.; Dolphin, D. In *The Chemical and Physical Behavior of Porphyrin Compounds and Related Structures*; Adler, A. D., Ed.; New York Academy of Sciences: New York, 1973; Vol. 206, pp 504−515.

(42) Spiro, T. G. In *Iron Porphyrins, Part II*; Lever, A. B. P., Gray, H. B., Eds.; Addison-Wesley: Reading, MA, 1983; p 110.

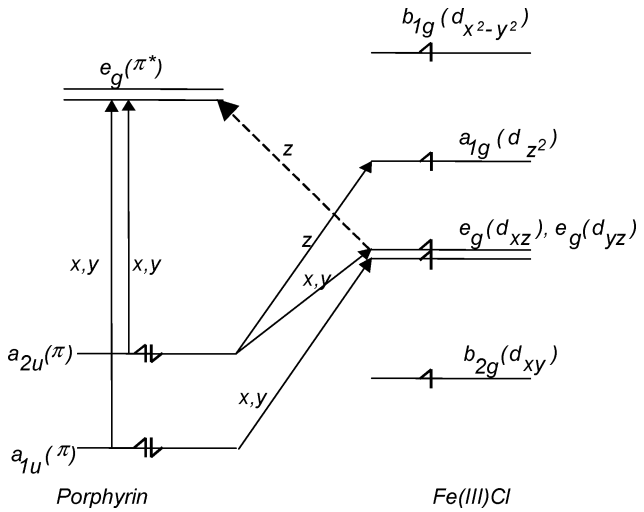

Figure 6. A qualitative molecular orbital diagram for the allowed transitions involving the Fe(III) and porphyrin orbitals for hemin based on the calculations by Zerner et al.[38] Characteristic bands (I−IV) are indicated, along with their respective polarizations. The dashed arrow indicates the assignment of the *z*-polarized transition centered at 867 nm in β-hematin. This complex belongs to the C_{4v} point group; however, the symmetry labels are for D_{4h}.

et al.[38] Hitherto no *z*-polarized transition has been reported for high-spin ferric hemes in the 800−1000 nm region; however, such *z*-polarized transitions have been predicted using a semiempirical quantum chemical INDO/ROHF/CI method.[43] Transitions that are *z*-polarized have been observed for high-spin four-coordinate ferrous hemes, including deoxyhemoglobin and deoxymyoglobin. Eaton et al.[44] assigned four bands within the near-infrared region to CT and d−d transitions for high-spin deoxyHb, which has the same effective symmetry (C_{4v}) as hemin. These include band I ($d_{xz} \rightarrow e_g(\pi^*)$) at 917 nm, band II ($d_{xz} \rightarrow d_{z^2}$ or $a_{2u}(\pi) \rightarrow d_{x^2-y^2}$) at 813 nm, band III ($a_{2u}(\pi) \rightarrow e_g(d_{yz})$) at 762 nm, and band IV ($a_{1u}(\pi) \rightarrow e_g(d_{yz})$) at 671 nm.

Band III has attracted considerable attention because of its sensitivity to protein conformational changes in response to bond breaking and recombination.[44−46] The position of band III is assumed to be related to the out-of-plane position of the Fe. On the basis of the B-term MCD spectrum, band III is assigned to the $a_{1u}(\pi) \rightarrow e_g(d_{yz})$ transition.[44] In the case of hemin and β-hematin, excitation at 564, 780, and 830 nm resulted in dramatic enhancement of A_{1g} and moderate enhancement of some B_{1g} modes. The inclusion of A_{1g} modes suggests that the mechanism is different from that reported by Franzen et al.[47] for Raman measurements of deoxyHb when exciting in the band III region. In terms of local coordinates, it is interesting to note that the majority of bands enhanced include out-of-plane vibrations, pyrrole folds, pyrrole breathing modes, and the Fe−N local coordinate. Because of the C_{4v} effective symmetry, most of these modes involve electronic displacement mainly along the *z*-axis of the porphyrin, thus inducing charge displacement along this axis, which can theoretically result in band enhancement. Exciting with the 564-nm laser line produced a similar profile to the 830-nm spectrum, both showing the enhancement of totally symmetric A_{1g} modes. Consequently, the band centered at ~550 nm in the UV−visible spectrum of hemin and β-hematin is tentatively assigned to a vibronically allowed *Q* (1,0) *z*-polarized transition $a_{2u}(\pi) \rightarrow d_{z^2}$.

The band centered at 867 nm in hemin and β-hematin appears to have characteristics to suggest that the enhancement results predominantly from a band I type transition $d_{xz} \rightarrow e_g(\pi^*)$. However, enhancement from other bands in the vicinity cannot be eliminated until complete near-IR Raman excitation profiles and MCD data are available. Factors that support the assignment of the 867-nm transition to band I include:

(1) Band I is an electric dipole allowed small broad band located between 800 and 1000 nm for high-spin hemes.

(2) The strong enhancement of A_{1g} modes, out-of-plane modes, and some pyrrole-breathing and deformation normal modes is indicative of a *z*-polarization transition that is a characteristic of band I.

(3) Band I has an excited electronic state configuration that corresponds to the direct product $E \times E = A_1 + A_2 + B_1 + B_2$, which cannot mix with the excited state configuration of the Soret transition. Thus, band I cannot vibronically couple to the Soret band. Consequently, one would expect totally symmetric A_1 modes (A_1 in C_{4v}) to be enhanced as predicted by the Albrecht formalism.[12,48]

4) The stacking of hemes should result in strong excitonic interactions for *z*-polarized transitions as verified by the intensity of the A_{1g} modes in β-hematin compared to hemin at near-infrared excitation wavelengths.

It has been predicted that excitation of charge-transfer bands should allow resonance of iron−ligand and iron−nitrogen stretching modes because both the transition moments of these bands and the vibrational modes are perpendicular (or *z*-polarized) relative to the porphyrin plane.[49,50] Asher et al.[51] observed resonant Raman enhancement of low wavenumber modes in metHb when exciting in the 600−630-nm region. Consequently, the band observed at 867 nm in hemin and β-hematin must have charge-transfer character. The enhancement of A_{1g} modes and low wavenumber out-of-plane modes are even more pronounced in hemozoin and β-hematin compared to hemin at excitation wavelengths 568, 780, and 830 nm. This provides an important insight into the mechanism of enhancement. This additional enhancement observed in the oligomeric hemes results from excitonic coupling between covalently bonded hemes in the extended porphyrin array. The porphyrin array enables delocalized electrons to migrate between porphyrins either covalently via the propionate linkage or noncovalently through van der Waals contacts or alternatively through space. The oscillatory field necessary to induce a dipole moment in this extended porphyrin array may interact with long excitation wavelengths, thus providing a plausible explanation for the extraordinary enhancement observed at 780- and 830-nm excitation. The presence of enhanced low-wavenumber bands for the aggregated porphyrin can be attributed to intermolecular

(43) Harris, D.; Loew, G. *J. Am. Chem. Soc.* **1993**, *115*, 5799−5802.
(44) Eaton, W. A.; Hanson, L. K.; Stephens, P. J.; Sutherland, J. C.; Dunn, J. B. R. *J. Am. Chem. Soc.* **1978**, *100*, 4991−5003.
(45) Ansari, A.; Jones, C. M.; Henry, E. R.; Hofrichter, J.; Eaton, W. A. *Science* **1992**, *256*, 1796−1798.
(46) Lim, M.; Jackson, T. A.; Anfinrud, P. A. *Proc. Natl. Acad. Sci. U.S.A.* **1993**, *90*, 5801−5804.
(47) Franzen, S.; Wallace-Williams, S. E.; Shreve, A. P. *J. Am. Chem. Soc.* **2001**, *124*, 7146−7155.
(48) We acknowledge one of the reviewers for this important symmetry argument.
(49) Spiro, T. G. *Biochim. Biophys. Acta* **1975**, *416*, 19−189.
(50) Desbois, A.; Lutz, M.; Banerjee, R. *Biochemistry* **1979**, *18*, 1510−1518.
(51) Asher, S. A.; Vickery, L. E.; Schuster, T. M.; Sauer, K. *Biochemistry* **1977**, *16*, 5849−5856.

vibrational modes in the aggregate formation direction (the out-of-plane or *z*-direction) and is precisely the conclusion reached through the AERS quantum theoretical scheme advanced by Akins et al.[13] The enhancement is much more pronounced in *β*-hematin compared to monomeric hemin; however, the hemin aggregate does exhibit some enhancement at near-IR excitation wavelengths. This enhancement could also be attributed to excitonic interactions between closely packed porphyrins in the hemin crystal. In this case the excitonic coupling could occur "through space" or alternatively between van der Waals contacts and not require a direct covalent linkage. The structure of hemin consists of a pair of Fe(PP-IX) units linked by carboxylic bonds and has the same space group as hemozoin, $P\bar{1}$, but with a different unit cell volume.[28] The close packing of hemin in the crystal could facilitate such excitonic interactions, explaining the enhancement of the totally symmetric modes at longer wavelengths. The fact that the enhancement is greater in *β*-hematin compared to that in hemin suggests the porphyrins are closer in the *β*-hematin compared to the hemin as a direct consequence of the propionate linkage. Further supporting the excitonic coupling hypothesis is the small red-shift of the band at 867 nm as the hemin is converted to *β*-hematin. More work on model compounds including heme dimers, trimers, and tetramers is required to ascertain whether the enhancement observed in hemin is primarily the result of excitonic interactions or solely due to exciting into the broad *z*-polarized charge-transfer band centered at 867 nm.

Structure of *β*-Hematin. Recent high-resolution powder diffraction data indicate that the structure *β*-hematin is a hydrogen-bonded chain of reciprocating dimers with each porphyrin within the dimer linked together by a propionate linkage.[5] The high number of diffraction peaks (150) along with the relatively low *R*-factor ($R_{wp} = 6.75\%$) indicates a reliable fit.[52] However, the precise position of some atoms still remains uncertain, and during the Rietveld refinement the propionic acid dimer was found to have discernible deviation from planarity.[53] Bohle et al.[54] addressed this aspect by performing density functional calculations for the gas phase formic acid dimer. They suggested that if the propionic acid group is deformed and nonplanar, then a Raman band at approximately 1712 cm^{-1} and an IR band at approximately 1625 cm^{-1} would be observed. This is because any reduction in symmetry from centrosymmetric C_{2h} point to C_{2v} or C_2 would be expected to lift the mutual exclusion of both bands. FTIR microspectroscopic measurements of *β*-hematin and hemozoin reveal a previously unreported carbonyl band at 1742 cm^{-1}. The Raman spectra of these compounds when excited with 564, 633, 830, and 1064-nm excitation displayed weak bands in the vicinity of 1750−1720 cm^{-1}. The appearance of bands within the 1750−1720 cm^{-1} region in both the FTIR and Raman spectra indicates at least one other carbonyl environment exists in *β*-hematin and hemozoin. The small size of these bands indicates that the carbonyl group is not associated with the bulk of the compound and is probably the result of surface carboxylates at either grain or surface boundaries.[55]

Conclusion

This study provides new insight into the electronic structure of the high-spin ferric complexes hemin, *β*-hematin, and hemozoin. The dramatic enhancement of totally symmetric A_{1g} modes at 780- and 830-nm excitation wavelengths observed in the spectra of *β*-hematin indicates the existence of a *z*-polarized charge-transfer band. Optical spectroscopic measurements recorded during the synthesis of *β*-hematin from hemin show a small broad band in this vicinity. On the basis of the Raman excitation profile of *β*-hematin, the UV−vis spectrum, and symmetry considerations, the band at 867 nm is assigned to the CT band $d_{xy} \rightarrow e_g(\pi^*)$. Because the Raman band enhancement was much greater in *β*-hematin compared to that in monomeric hemin, it is suggested that the additional enhancement is the result of excitonic coupling between covalently linked porphyrins in the aggregated array. This is especially relevant because the stacking of hemes should result in strong interactions for *z*-polarized transitions. To provide more insight into the enhancement mechanism, an investigation into model compounds including heme *μ*-oxo-dimers, trimers, and tetramers is currently underway in our laboratory. This study has important implications in understanding the structure and formation of malaria pigment. Such information will be useful for the urgently required development and testing of novel therapeutic agents for the treatment of prophylaxis of human malaria infections.

Acknowledgment. This work is supported by an Australian Research Council Large Grant (DP0450573). Dr. Cooke is supported by the National Health and Medical Research Council of Australia and is a recipient of grants from the National Institute of Health (NIH, Grants DK32094-10 and A144008-04A1). We thank Prof. Robert Armstrong and Dr. Elizabeth Carter (School of Chemistry, University of Sydney) for use of the Spectra Physics Ar^+ Stabilite 2017 laser system, Spectra-Physics Kr^+ Beamlock 2060 laser, 830-nm diode laser, FT-Raman instrument, and for general assistance in taking measurements with these systems. We thank Ewen Smith (Department of Pure and Applied Chemistry, University of Strathclyde) for use of the 406-nm laser coupled to the Raman 2000 system. We also thank Mr. Finlay Shanks (Monash University) for instrument support and maintenance.

Supporting Information Available: Table depicting band assignments, local coordinates, relative band intensities, and symmetry terms for *β*-hematin and Raman spectra of hemin recorded using the same excitation wavelengths as those applied to *β*-hematin except for 1064 nm because this spectrum has previously been reported in ref 34. This material is available free of charge via the Internet at http://pubs.acs.org.

JA038691X

(52) Egan, T. J. *J. Inorg. Biochem.* **2002**, *91*, 19−26.
(53) Harris, K. D. M.; Tremayne, B. M.; Kariuki, B. M. *Angew. Chem., Int. Ed.* **2001**, *40*, 1626−1651.
(54) Bohle, D. S.; Kosar, A. D.; Madsen, S. K. *Biochem. Biosphys. Res. Commun.* **2002**, *294*, 132−135.

(55) We acknowledge one of the reviewers for suggesting surface carboxylates as an explanation for the band appearing at ~1742 cm^{-1} in the FTIR spectra.